



# Hydrothermal Synthesis of Fine NaTaO<sub>3</sub> Powder as a Highly Efficient Photocatalyst for Overall Water Splitting

Yungi Lee,<sup>1</sup> Tomoaki Watanabe,<sup>3</sup> Tsuyoshi Takata,<sup>1</sup> Michikazu Hara,<sup>2</sup>  
Masahiro Yoshimura,<sup>3</sup> and Kazunari Domen<sup>\*1,4</sup>

<sup>1</sup>Department of Chemical System Engineering, The University of Tokyo, 7-3-1 Hongo, Bunkyo-ku, Tokyo 113-8656

<sup>2</sup>Chemical Resources Laboratory, Tokyo Institute of Technology, 4259 Nagatsuta, Midori-ku, Yokohama 226-8503

<sup>3</sup>Materials and Structures Lab., Tokyo Institute of Technology, 4259 Nagatsuta, Midori-ku, Yokohama 226-8503

<sup>4</sup>Solution-Oriented Research for Science and Technology (SORST), Japan Science and Technology Co. (JST),  
2-1-13 Higashiueno, Taito-ku, Tokyo 110-0015

Received June 29, 2006; E-mail: domen@chemsys.t.u-tokyo.ac.jp

A fine powder of sodium tantalum(V) trioxide as single-phase perovskite NaTaO<sub>3</sub> has been successfully prepared by hydrothermal synthesis through the reaction of a sodium hydroxide solution and ditantalum pentaoxide powder at low temperature (373–473 K). The NaTaO<sub>3</sub> powder has high photocatalytic activity for both H<sub>2</sub> evolution (8.0 mmol h<sup>−1</sup>) and O<sub>2</sub> evolution (4.1 mmol h<sup>−1</sup>), which is attributed to the high surface area, small particle size and high crystallinity of the powder catalyst.

Perovskite-type sodium tantalate (NaTaO<sub>3</sub>) has been reported to be a highly efficient photocatalyst for overall water splitting under ultraviolet (UV) irradiation.<sup>1</sup> The preparation of NaTaO<sub>3</sub> has been successfully achieved through a variety of methods, including sol–gel synthesis,<sup>2</sup> alkalide reduction,<sup>3</sup> plasma-electrochemical synthesis,<sup>4</sup> hydrothermal–electrochemical synthesis,<sup>5</sup> and a conventional solid-state reaction. Among these preparation methods, the solid-state reaction at high temperature (1423 K) is generally employed when a crystalline form of the photocatalyst is required. However, sintering at high temperatures results in a powder with a large particle size and low surface area. Doping with lanthanum has been investigated as a means of reducing the particle size and improving photocatalytic activity.<sup>6</sup> Lowering the reaction temperature in the preparation of the NaTaO<sub>3</sub> powder has also been considered in an attempt to obtain small grain size and high surface area.

Hydrothermal synthesis is an effective method for preparing crystalline ceramic powders at moderate temperature.<sup>7</sup> In addition to the moderate synthesis conditions, hydrothermal synthesis provides easy control of geometric properties, such as surface morphology, surface area, and particle size, through the appropriate selection of starting materials and simple adjustment of synthesis conditions, i.e., temperature, time, and mixing ratio. TiO<sub>2</sub>, a well-known photocatalyst, prepared by hydrothermal synthesis<sup>8</sup> or the hydrothermal crystallization in organic media (HyCOM) method,<sup>9,10</sup> has high surface area and high crystallinity. This catalyst exhibits high photocatalytic activity in various reactions, including the mineralization of acetic acid, silver-metal deposition, and hydrogen evolution from methanol solution. He et al. reported that nano-sized NaTaO<sub>3</sub> powder, prepared by hydrothermal methods at low temperature, exhibits high photocatalytic activity for the deg-

radation of gaseous formaldehyde and rhodamine B solution.<sup>11</sup>

In this study, NaTaO<sub>3</sub> powder is prepared by hydrothermal synthesis through reaction between commercial Ta<sub>2</sub>O<sub>5</sub> powder and NaOH solution under various synthesis conditions. The prepared NaTaO<sub>3</sub> powder samples have been fully characterized, and the photocatalytic activity for overall water splitting has been investigated.

## Experimental

**Preparation.** NaTaO<sub>3</sub> powder was prepared by hydrothermal synthesis as follows. The starting material Ta<sub>2</sub>O<sub>5</sub> (>99.5%, Kanto Chemical) was dissolved in 100 mL of NaOH (>97.0%, Kanto Chemical) aqueous solution with concentrations in the range of 0.6–40 M. A Teflon beaker containing the solution was placed in an autoclave and then treated hydrothermally at temperatures from room temperature to 473 K for periods of 3–90 h. The synthesized powder was taken from the autoclave after cooling to room temperature, and all solid residues were separated by filtration. The desired products were washed with water and dried in air prior to characterization and photocatalytic reaction. The samples were calcined at the desired temperature for 3 h and then cooled down to the room temperature. For comparison, NaTaO<sub>3</sub> was prepared by solid-state reaction by calcination of a mixture of Na<sub>2</sub>CO<sub>3</sub> (99.5%, Kanto Chemical) and Ta<sub>2</sub>O<sub>5</sub> (>99.5%, Kanto Chemical) at 1423 K for 10 h in the presence of excess (5%) sodium to avoid volatilization.<sup>12</sup>

**Characterization.** The structures were characterized by X-ray diffractometry (XRD; RINT 2100, Rigaku) using Cu K $\alpha$  radiation at 40 kV and 40 mA. The XRD patterns were collected at 2 $\theta$  angles of 10–80° at a scan rate of 4° min<sup>−1</sup>. The surface morphologies and average particle sizes of the products were observed by field-emission scanning electron microscopy (SEM; S-4700, Hitachi) and field-emission transmission electron microscopy (TEM; JEM-2010F, JEOL). The surface areas were determined

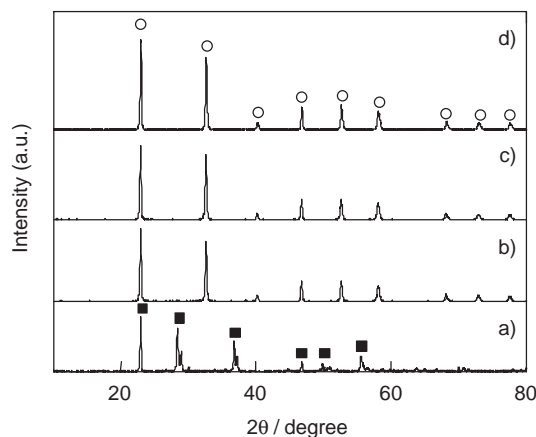


Fig. 1. XRD patterns of  $\text{NaTaO}_3$  powders prepared by hydrothermal synthesis in 10 M NaOH solution for 24 h at (a) room temperature, (b) 373 K, (c) 423 K, and (d) 473 K. Squares denote  $\text{Ta}_2\text{O}_5$  and circles denote  $\text{NaTaO}_3$ .

by Brunauer–Emmett–Teller (BET) measurements (SA3100, Coulter). The sodium and tantalum contents of the samples were analyzed by energy-dispersive X-ray spectroscopy (EDX; EMAX 7000, Horiba). Thermogravimetric and differential thermal analysis (TG-DTA; DTG-50H, Shimadzu) was performed to determine the water content of the powders using ca. 20 mg of sample by heating at  $10\text{ K min}^{-1}$  to 1373 K under air flow at  $50\text{ mL min}^{-1}$ . Photoluminescence measurements were conducted using a spectrofluorometer (FP-660, Jasco) with a 200 W Xe lamp at 77 K.

**Photocatalytic Reaction.** Photocatalytic reactions were carried out in a closed gas circulation system. The  $\text{NaTaO}_3$  powder (0.3 g) was dispersed in distilled water in a reaction vessel using a magnetic stirrer. Prior to reaction, the system was degassed and then filled with a small amount of Ar gas (30 torr). A 450 W high-pressure mercury lamp (UM-452, Ushio) was used as the light source in an internal irradiation-type quartz jacket. The quantities of evolved gases were determined by gas chromatography with thermal conductivity detector (GC-8A, Shimadzu; Ar carrier gas). The powder was also loaded with  $\text{Ni}(\text{NO}_3)_2 \cdot 6\text{H}_2\text{O}$  (>98.0%, Kanto Chemical) by impregnation, and the resultant mixture was calcined in air at 543 K for 1 h prior to reaction and then oxidized as a NiO cocatalyst.

## Results and Discussion

**Preparation of  $\text{NaTaO}_3$  Photocatalyst by Hydrothermal Synthesis.** Figure 1 shows the XRD patterns of the samples prepared in 10 M NaOH solution at various temperatures with a synthesis time of 24 h. All peaks produced by the sample synthesized at room temperature are assigned to the starting material  $\text{Ta}_2\text{O}_5$ , indicating that the phase was unchanged even after hydrothermal treatment for 24 h. A single phase of  $\text{NaTaO}_3$  was obtained at temperatures greater than 373 K, and no other by-products were detected under any of these conditions. The half-width of the XRD peaks for each product decreased as the synthesis temperature was increased from 373 to 473 K, indicating an increase in crystallinity. The TG-DTA results show complete dehydration (broad endothermic peaks at ca. 373 and 673 K), accompanied by slight weight losses due to loss of crystal water and/or hydroxy groups in the synthesized  $\text{NaTaO}_3$  powder. The slight weight loss in the present product indicates that the hydrothermally synthesized powder

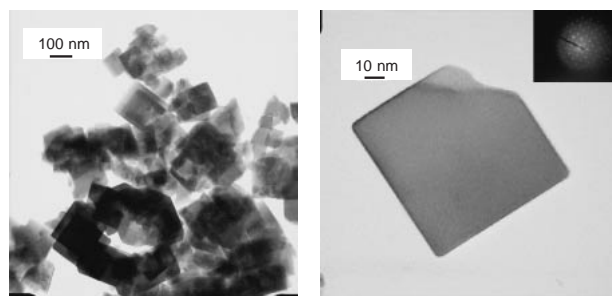


Fig. 2. TEM images and electron diffraction pattern (inset) of  $\text{NaTaO}_3$  powder prepared by hydrothermal synthesis in 10 M NaOH solution for 24 h at 423 K.

Table 1. BET Surface Areas and Photocatalytic Activities of  $\text{NaTaO}_3$  Powders Prepared by Hydrothermal Synthesis in 10 M NaOH Solution for 24 h at Various Synthesis Temperatures

Synthesis temp/K	BET surface area/ $\text{m}^2\text{ g}^{-1}$	Photocatalytic activity <sup>a)</sup>	
		$\text{H}_2/\text{mmol h}^{-1}$	$\text{O}_2/\text{mmol h}^{-1}$
373	4.6	0.1	n.d.
423	5.0	1.2	0.6
473	4.3	6.0	3.0

a) With NiO (0.2 wt %) loaded as a cocatalyst.

is not afforded in a hydrated state. TEM images of the  $\text{NaTaO}_3$  powder prepared at 423 K over 24 h in 10 M NaOH solution are shown in Fig. 2. The powder consists of well-crystallized primary particles with size of ca. 100 nm (Fig. 2b). However, the primary particles are aggregated (Fig. 2a), which appears to occur during the hydrothermal process. The electron diffraction pattern displays clear spots, indicative of the good crystallinity of the prepared  $\text{NaTaO}_3$  powder. The synthesized  $\text{NaTaO}_3$  powder has a Na/Ta ratio of 1, as confirmed by elemental analysis, suggesting that no sodium defects are present in the bulk of the hydrothermally synthesized  $\text{NaTaO}_3$  powder. Table 1 shows the photocatalytic activities of the samples prepared at various synthesis temperatures and the respective BET surface areas. The BET surface area of each sample is almost the same ( $5.0\text{ m}^2\text{ g}^{-1}$ ) regardless of the synthesis temperature. However, the  $\text{NaTaO}_3$  photocatalyst that was prepared at 473 K displayed the highest photocatalytic activity, which is 4 times that of the powder synthesized at 423 K and 60 times that of the powder prepared at 373 K. The  $\text{NaTaO}_3$  photocatalyst prepared at 473 K decomposed water into  $\text{H}_2$  and  $\text{O}_2$  at a stoichiometric ratio with activities of  $6.0\text{ mmol h}^{-1}$  for  $\text{H}_2$  evolution and  $3.0\text{ mmol h}^{-1}$  for  $\text{O}_2$  evolution. The high photocatalytic activity of this powder is probably due to its high crystallinity, as confirmed by XRD measurements.

Samples prepared by hydrothermal synthesis in 10 M NaOH solution at 423 K did not exhibit significant differences in XRD measurements, regardless of synthesis time. All of the detected peaks have been assigned to the perovskite  $\text{NaTaO}_3$  phase, even for the sample synthesized for only 3 h. The BET surface areas and photocatalytic activities of these samples are listed in Table 2. The BET surface areas of all these  $\text{NaTaO}_3$  powders are close to  $5.0\text{ m}^2\text{ g}^{-1}$ . However, the photocatalytic activity for water splitting increased with synthesis time. The

Table 2. BET Surface Areas and Photocatalytic Activities of NaTaO<sub>3</sub> Powders Prepared by Hydrothermal Synthesis at 423 K in 10 M NaOH Solution for Various Synthesis Times

Synthesis time/h	BET surface area/m <sup>2</sup> g <sup>-1</sup>	Photocatalytic activity <sup>a)</sup>	
		H <sub>2</sub> /mmol h <sup>-1</sup>	O <sub>2</sub> /mmol h <sup>-1</sup>
3	4.7	0.3	n.d.
24	5.0	1.2	0.6
90	5.7	2.0	1.0

a) With NiO (0.2 wt %) loaded as a cocatalyst.

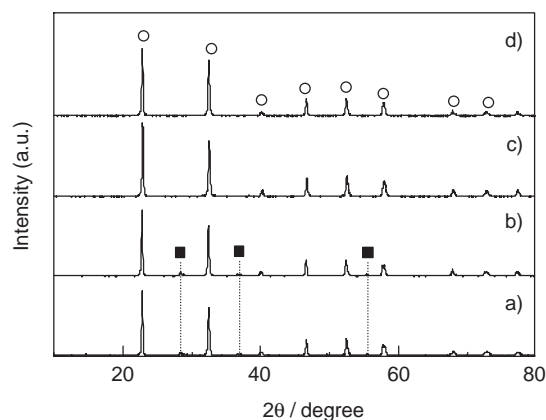


Fig. 3. XRD patterns of NaTaO<sub>3</sub> powders prepared by hydrothermal synthesis at 423 K for 24 h in NaOH solution at a concentration of (a) 0.6 M, (b) 2.5 M, (c) 5 M, and (d) 40 M. Squares denote Ta<sub>2</sub>O<sub>5</sub> and circles denote NaTaO<sub>3</sub>.

NaTaO<sub>3</sub> photocatalyst obtained by synthesis for 90 h exhibited the highest photocatalytic activity, i.e., it was 1.5 times higher than that for the product synthesized over 24 h and 6 times higher than that reacted for 3 h. Synthesis times of more than 24 h did not have any effect on the photocatalytic activities of the samples prepared at 473 K (50 K higher), indicating that the increase in photocatalytic activity with synthesis time is due to an increase in crystallinity for these samples.

Figure 3 shows the XRD patterns of samples prepared at 423 K for 24 h in various concentrations of NaOH. At lower NaOH concentrations (0.6 and 2.5 M), the Ta<sub>2</sub>O<sub>5</sub> phase was not completely transformed to NaTaO<sub>3</sub>, even after treatment for 24 h. NaOH concentrations exceeding 2.5 M are therefore necessary to convert Ta<sub>2</sub>O<sub>5</sub> quantitatively to perovskite NaTaO<sub>3</sub> powder. Figure 4 shows the surface morphologies of NaTaO<sub>3</sub> powder obtained by hydrothermal synthesis in solutions of various NaOH concentration. While all particles present a cubic shape, the average particle size decreases with increasing NaOH concentration up to 10 M, above which the particle size exhibits no further change. He et al. have reported that the formation of NaTaO<sub>3</sub> by reaction of Ta<sub>2</sub>O<sub>5</sub> powder in NaOH solution proceeds via a dissolution–precipitation mechanism,<sup>11</sup> which also occurs in the hydrothermal formation of perovskite materials, such as BaTiO<sub>3</sub>.<sup>13,14</sup> In the dissolution–precipitation mechanism, the concentration of the solvent (NaOH solution in this case) plays an important role in controlling the rate of nucleation and powder growth. As the NaOH concentration increases, the dissolution of ditantalum

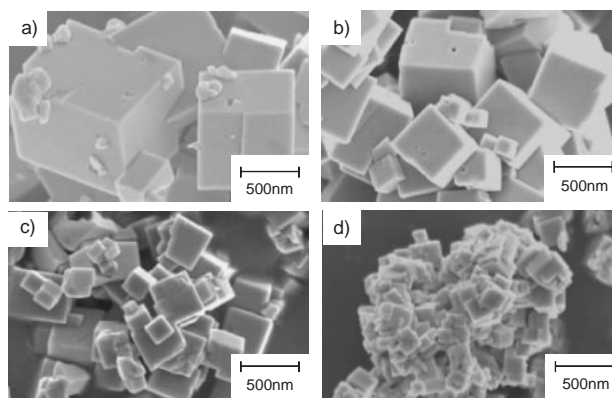


Fig. 4. SEM images of NaTaO<sub>3</sub> powders prepared by hydrothermal synthesis at 423 K for 24 h in NaOH solution at a concentration of (a) 0.6 M, (b) 2.5 M, (c) 5 M, and (d) 40 M.

Table 3. BET Surface Areas and Photocatalytic Activities of NaTaO<sub>3</sub> Powders Prepared by Hydrothermal Synthesis at 423 K for 24 h in NaOH of Various Concentrations

NaOH concentration/M	BET surface area/m <sup>2</sup> g <sup>-1</sup>	Photocatalytic activity <sup>a)</sup>	
		H <sub>2</sub> /mmol h <sup>-1</sup>	O <sub>2</sub> /mmol h <sup>-1</sup>
0.6	1.5	0.1	n.d.
2.5	1.7	0.5	0.2
10	5.0	1.2	0.6
40	5.6	1.7	0.9

a) With NiO (0.2 wt %) loaded as a cocatalyst.

pentaoxide precursors becomes more aggressive, resulting in more rapid nucleation and slow grain growth, and therefore, the average particle size is smaller. Above 10 M NaOH, however, the dissolution of the tantalum species from Ta<sub>2</sub>O<sub>5</sub> becomes the rate-controlling process, preventing any further decrease in average particle size regardless of the NaOH concentration. Table 3 shows the photocatalytic activities of samples prepared in various concentrations of NaOH and the respective BET surface areas. The BET surface area of the samples increase with NaOH concentration from 0.6 to 40 M, and the NaTaO<sub>3</sub> powder prepared in 40 M NaOH has a surface area 5 times that of the powder synthesized in 0.6 M NaOH. The photocatalytic activities of these samples (Table 3) also increase with NaOH concentration, which is attributed to the increase in surface area. However, further increase of NaOH concentration than 40 M did not affect the photocatalytic activity of the product.

The physical properties of the photocatalyst, such as surface area, particle size, and crystallinity, are closely related to photocatalytic activity.<sup>9,10</sup> It is thought that the surface area affects the number of sites, at which the photocatalytic reaction occurs, while the particle size influences the distance that photo-generated electrons and holes migrate from the bulk to reach the active sites. The crystallinity of the photocatalyst is related to the number of defects and vacancies, which act as recombination centers for the photogenerated electrons and holes. Thus, high surface area, small particle size, and high crystallinity are required to obtain high photocatalytic activity. In the

Table 4. BET Surface Areas and Photocatalytic Activities of Hydrothermally Synthesized NaTaO<sub>3</sub> Powders after Calcination at Various Temperatures

Calcination temp/K	BET surface area/m <sup>2</sup> g <sup>-1</sup>	Photocatalytic activity <sup>a)</sup> /mmol h <sup>-1</sup>	
		H <sub>2</sub>	O <sub>2</sub>
As-synthesized <sup>b)</sup>	5.7	2.0	1.0
573	6.3	1.6	0.8
973	3.2	1.5	0.7
1273	1.3	0.3	0.1

a) With NiO (0.2 wt %) loaded as a cocatalyst. b) Prepared in 10 M NaOH solution at 423 K for 90 h.

present hydrothermal synthesis, the physical properties of the products have been successfully controlled by the synthesis conditions. In other words, surface area and particle size are controlled by the concentration of the NaOH solution, and the crystallinity is controlled by the synthesis temperature and duration. A drastic increase of photocatalytic activity with increasing synthesis temperature, shown in Table 1, indicates that the crystallinity of the product is the main factor to determine the photocatalytic activity.

Table 4 lists the photocatalytic activity of the NaTaO<sub>3</sub> powders after calcination at various temperatures. There are several reports concerning the use of post-preparation calcination to control the physical properties, e.g., crystallinity and surface area, of nano-crystalline titanium dioxide synthesized by HyCOM.<sup>15,16</sup> Ohtani et al. reported that post-calcination resulted in a dramatic decrease in the second-order rate constants of electron-hole recombination, giving rise to an increase in photocatalytic activity.<sup>17</sup> Such an increase in photocatalytic activity is attributed to a decrease in the density of oxygen vacancies, and the accompanying increase in crystallinity. However, the photocatalytic activity of the present hydrothermally synthesized NaTaO<sub>3</sub> powder for overall water splitting remained unchanged upon calcination at temperatures lower than 1273 K, and calcination at higher temperature resulted in a dramatic decrease in photocatalytic activity for this reaction. This decrease in activity is attributable to an increase in the density of surface defects at grain boundaries as a result of high-temperature calcination.<sup>18,19</sup> The lack of any change in activity upon calcination at lower temperature suggests that hydrothermal synthesis affords NaTaO<sub>3</sub> powder with high crystallinity, that is, the structure is relatively free of oxygen vacancies without calcination. Tungsten trioxide and titanium dioxide powders prepared by hydrothermal synthesis were also found to exhibit high photocatalytic activity without post-calcination due to the high crystallinity of the hydrothermal product.<sup>8,19</sup>

Among the present samples, the NaTaO<sub>3</sub> powder prepared by hydrothermal synthesis at 473 K in 10 M NaOH solution for longer than 24 h, regardless of post-calcination, displayed the highest photocatalytic activity for overall water splitting. It is well known that photocatalytic activity is closely related to the type, loading state, and loading amount of cocatalyst. For NaTaO<sub>3</sub> photocatalysts prepared by a solid-state reaction, it has been reported that nickel oxide is an effective cocatalyst for overall water splitting reaction.<sup>20</sup> The dependence of activity on the loading amount of NiO for the optimal hydrother-

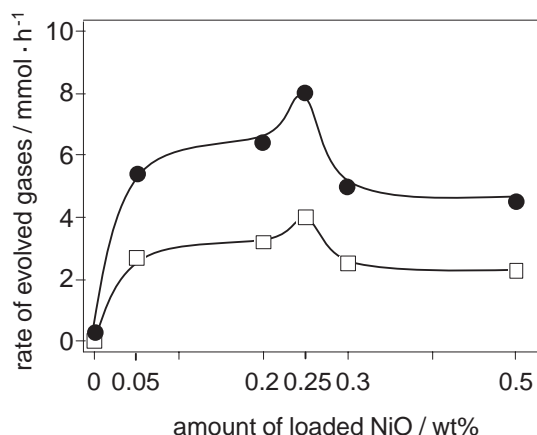


Fig. 5. Optimum loading of NiO for NaTaO<sub>3</sub> powder prepared in 10 M NaOH solution at 473 K for 24 h. Circles denote hydrogen evolution and squares denote oxygen production.

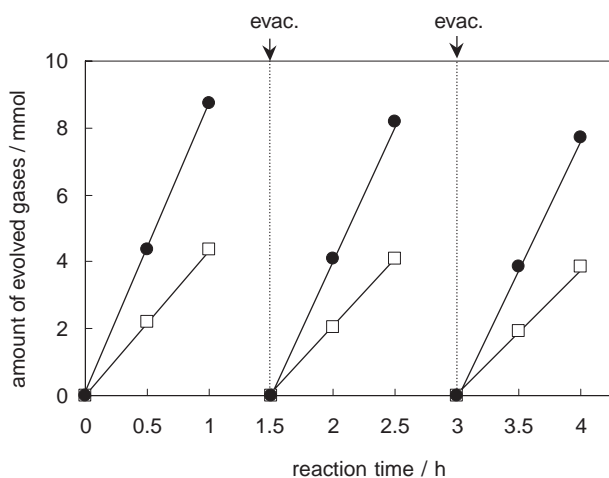


Fig. 6. Time courses of gas evolution for NaTaO<sub>3</sub> powder prepared in 10 M NaOH solution at 473 K for 24 h and loaded with 0.25 wt % NiO. Circles denote hydrogen evolution and squares denote oxygen production.

mally synthesized NaTaO<sub>3</sub> powder is shown in Fig. 5. The highest photocatalytic activity was obtained with 0.25 wt % NiO. Figure 6 shows the time course of H<sub>2</sub> and O<sub>2</sub> evolution over the NaTaO<sub>3</sub> powder loaded with 0.25 wt % NiO under UV irradiation. Stable photocatalytic performance was obtained using this catalyst system, and the H<sub>2</sub>/O<sub>2</sub> production ratio was stoichiometric (ratio of 2) within experimental error. Although the rate of H<sub>2</sub> and O<sub>2</sub> evolution in the second and subsequent runs with intermittent evacuation was slightly lower than in the first run, the reaction continued steadily with activities of ca. 8.0 mmol h<sup>-1</sup> for H<sub>2</sub> evolution and ca. 4.0 mmol h<sup>-1</sup> for O<sub>2</sub> evolution. The change in color of the NiO-loaded NaTaO<sub>3</sub> as a result of the reaction suggests that the slight decrease in photocatalytic activity in subsequent runs is due to a change in the state of the cocatalyst, from nickel oxide to nickel metal.<sup>11</sup> The total amount of H<sub>2</sub> and O<sub>2</sub> evolved over 3 h under UV irradiation was 37 mmol, greater than the amount of catalyst employed (0.30 g, 1.2 mmol



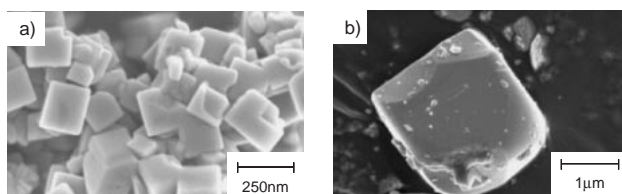


Fig. 7. SEM images of  $\text{NaTaO}_3$  powders prepared by a) hydrothermal synthesis prepared in 10 M NaOH solution at 473 K for 24 h and b) solid-state reaction.

Table 5. Band Gaps, BET Surface Areas, Cocatalyst Loadings, and Photocatalytic Activities of  $\text{NaTaO}_3$  Powders Prepared by a) Hydrothermal Synthesis and b) Solid-State Reaction

Sample	Band gap /eV	BET surface area / $\text{m}^2 \text{g}^{-1}$	Cocatalyst, NiO /wt %	Photocatalytic activity/ $\text{mmol h}^{-1}$	
				$\text{H}_2$	$\text{O}_2$
HT	4.1	5.0	0.25	8.8	4.4
SSR	4.0	0.3	0.05	1.1	0.4

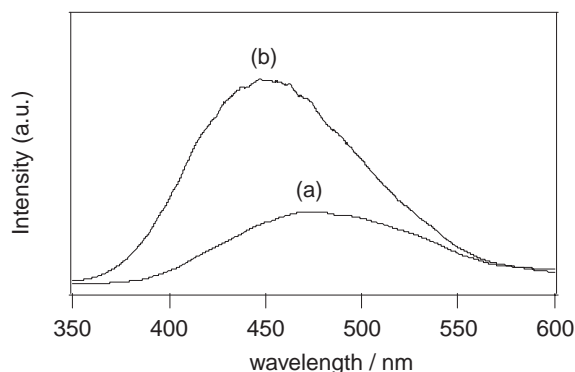


Fig. 8. Photoluminescence spectra at 77 K of  $\text{NaTaO}_3$  powders prepared by a) hydrothermal synthesis and b) solid-state reaction (excitation: 260 nm).

$\text{NaTaO}_3$ ). The XRD pattern of the catalyst did not change as a result of the reaction.

**Comparison with  $\text{NaTaO}_3$  Powder Prepared by Solid-State Reaction.** SEM images of  $\text{NaTaO}_3$  powder catalysts prepared by hydrothermal synthesis (HT) and solid-state reaction (SSR) are shown in Fig. 7. The HT sample consists of aggregates of primary particle with average size of ca. 100–200 nm. In contrast, the particles produced by the solid-state reaction are 10–20 times larger (average particle size: 1–2  $\mu\text{m}$ ). This result is reflected in the BET surface areas: 5.0  $\text{m}^2 \text{g}^{-1}$  for the former and 0.3  $\text{m}^2 \text{g}^{-1}$  for the latter (Table 5). The difference in average particle size and BET surface area most likely corresponds to the difference in synthesis temperature (473 K for HT vs 1423 K for SSR). Figure 8 shows the photoluminescence spectra at 77 K of powders prepared by both methods. The luminescence intensity of the HT powder is lower than that of the SSR powder, indicating that the former has a slightly higher density of sodium defects near the surface, which act as non-radioactive transition centers.<sup>12</sup> Sodium defects in the HT powder might be formed to compensate for proton defects due to the existence of  $\text{OH}^-$  ions in the

lattice. A similar result was reported for the hydrothermally prepared barium titanate by Hennings et al.<sup>20</sup> The HT powder exhibits peak photocatalytic activity when loaded with 0.25 wt % NiO, whereas only 0.05 wt % NiO<sup>21</sup> is required to achieve peak activity for the SSR powder. The difference in the optimum loading amount of cocatalyst can be attributed to the difference in surface area. As shown in the table, the peak photocatalytic activity for water splitting over the HT catalyst is 8 times higher than over the SSR catalyst. It is considered that the smaller particle size and higher surface area of the present catalyst increases the probability of surface reaction between electrons and holes rather than recombination in the bulk, resulting in high photocatalytic activity for overall water splitting despite the slightly elevated density of surficial sodium defects.

## Conclusion

A fine powder of sodium tantalum(V) trioxide as single-phase perovskite  $\text{NaTaO}_3$  was successfully synthesized by using a hydrothermal method at low temperature (373–473 K). The powder was prepared by the reaction of commercially available  $\text{Ta}_2\text{O}_5$  powder with NaOH solution, which occurs via a dissolution–precipitation mechanism. Experimental results showed that the concentration of the NaOH solution is the most important factor controlling the phase, particle size and morphology of the synthesized products in the sodium tantalate system. It was also shown that the synthesis temperature, which affects the crystallinity of the products, is the most significant factor affecting the photocatalytic activity of the catalyst.  $\text{NaTaO}_3$  powder obtained by hydrothermal synthesis was shown to be a highly efficient photocatalyst achieving stoichiometric water decomposition into  $\text{H}_2$  and  $\text{O}_2$  under UV irradiation. Photocatalytic activity as high as 8.0  $\text{mmol h}^{-1}$   $\text{H}_2$  and 4.1  $\text{mmol h}^{-1}$   $\text{O}_2$  was obtained from photocatalytic water splitting over  $\text{NaTaO}_3$  powder synthesized at 473 K in 10 M NaOH solution for longer than 24 h and loaded with 0.25 wt % NiO as a cocatalyst. This  $\text{NaTaO}_3$  powder exhibits photocatalytic activity 8 times higher than that for the corresponding catalyst prepared by solid-state reaction due to the higher surface area, smaller particle size, and higher crystallinity.

This research was supported by the Solution-Oriented Research for Science and Technology (SORST) program of the Japan Science and Technology Corporation (JST).

## References

- 1 H. Kato, K. Asakura, A. Kudo, *J. Am. Chem. Soc.* **2003**, 125, 3082.
- 2 M. D. Aguas, I. P. Parkin, *J. Mater. Sci. Lett.* **2001**, 20, 57.
- 3 J. A. Nelson, M. J. Wagner, *J. Am. Chem. Soc.* **2003**, 125, 332.
- 4 F. Schlottig, J. Schreckenbach, G. Marx, *Fresenius' J. Anal. Chem.* **1999**, 363, 209.
- 5 Y. Lee, T. Watanabe, T. Takata, J. N. Kondo, M. Hara, M. Yoshimura, K. Domen, *Chem. Mater.* **2005**, 17, 2422.
- 6 A. Kudo, H. Kato, *Chem. Phys. Lett.* **2000**, 331, 373.
- 7 K. Byrappa, M. Yoshimura, *Handbook of Hydrothermal Technology: A Technology for Crystal Growth and Materials Processing*, Noyes Publications, New Jersey, U.S.A., **2001**.

- 8 H. Hayashi, K. Torii, *J. Mater. Chem.* **2002**, *12*, 3671.
- 9 H. Kominami, S. Murakami, J. Kato, Y. Kera, B. Ohtani, *J. Phys. Chem. B* **2002**, *106*, 10501.
- 10 H. Kominami, T. Matsuura, K. Iwai, B. Ohtani, S. Nishimoto, Y. Kera, *Chem. Lett.* **1995**, 693.
- 11 Y. He, Y. Zhu, N. Wu, *J. Solid State Chem.* **2004**, *177*, 3868.
- 12 H. Kato, A. Kudo, *J. Phys. Chem. B* **2001**, *105*, 4285.
- 13 J. O. Eckert, Jr., C. C. Hung-Houston, B. L. Gersten, M. M. Lencka, R. E. Riman, *J. Am. Ceram. Soc.* **1996**, *79*, 2929.
- 14 N. A. Ovramenko, L. I. Shvets, F. D. Ovcharenko, B. Y. Kornilovich, *Izv. Akad. Nauk USSR, Neorg. Mater.* **1979**, *15*, 1982.
- 15 H. Kominami, Y. Takada, H. Yamagiwa, Y. Kera, M. Inoue, T. Inui, *J. Mater. Sci. Lett.* **1996**, *15*, 197.
- 16 H. Kominami, M. Kohno, Y. Takata, M. Inoue, T. Inui, Y. Kera, *Ind. Eng. Chem. Res.* **1999**, *38*, 2925.
- 17 B. Ohtani, R. M. Bowman, D. P. Colombo, Jr., H. Kominami, H. Noguchi, K. Uosaki, *Chem. Lett.* **1998**, 579.
- 18 P. T. Landsberg, *Recombination in Semiconductors*, Cambridge University Press, Cambridge, **1991**, p. 208.
- 19 H. Kominami, K. Yabutani, T. Yamamoto, Y. Kera, B. Ohtani, *J. Mater. Chem.* **2001**, *11*, 3222.
- 20 D. F. K. Hennings, C. Metzmacher, B. S. Schreinemacher, *J. Am. Ceram. Soc.* **2001**, *84*, 179.
- 21 H. Kato, A. Kudo, *Catal. Lett.* **1999**, *58*, 153.